1st Croatian Conference on Earthquake Engineering
1CroCEE
22-24 March 2021 Zagreb, Croatia

DOI: https://doi.org/10.5592/CO/1CroCEE.2021.71

Using regional earthquake risk models as priors to dynamically assess the impact on residential buildings after an event

Lukas Bodenmann[1], Yves Reuland[2], Božidar Stojadinović[3]

[1] *PhD candidate*, Dept. of Civil, Environmental and Geomatic Engineering, ETH Zurich, b*odenmann@ibk.baug.ethz.ch*

[2] *Senior researcher*, Dept. of Civil, Environmental and Geomatic Engineering, ETH Zurich, reuland@ibk.baug.ethz.ch

[3] *Professor*, Dept. of Civil, Environmental and Geomatic Engineering, ETH Zurich, *stojadinovic@ibk.baug.ethz.ch*

Abstract

Earthquakes can lead to widespread damage to the built environment, affecting many residential buildings and expose their residents to potentially severe and long-lasting physical and financial stress. While emergency response actions are still ongoing in the aftermath of such an event, public officials already have to take first decisions that will shape the reconstruction process and affect long-term societal consequences. Apart from the intense time pressure, this decision environment is characterized by the sparsity of available information on the amount and the spatial distribution of earthquake-triggered damage.

In this situation, regional earthquake risk models provide valuable first rapid impact predictions that are, however, typically associated with large uncertainties. Conversely, the amount and the spatial coverage of event-specific impact data increases during post-earthquake response and recovery. By leveraging probabilistic machine learning tools, the framework presented in this study makes it possible to benefit from the continuous data inflow to dynamically update the initial regional earthquake risk predictions and to constrain the associated model uncertainties. Whereas it might take several weeks until a first rapid visual safety screening is completed for all buildings in the earthquake-affected region, this study shows how data from only the first few screened buildings can substantially increase the quality of information available to decision-makers. This enables not only to predict outcomes of an ongoing building safety screening process, for example, predict the number of uninhabitable buildings, but also to constrain prior estimates for subsequent processes of the recovery phase, such as detailed damage assessments and reconstruction cost and time estimation. The presented framework is applied to a case-study region with 34000 residential buildings providing home to 500000 people that is subjected to a fictitious earthquake scenario.

Key words: Dynamic post-earthquake damage assessment, Regional earthquake-risk models, Housing resilience, Gaussian Process classification

1 Introduction

Earthquakes strike at random locations with unpredictable magnitude and spectral content, but with high destructive potential. Varying seismic design levels and material degradation of existing buildings add uncertainty to the damage and, by extension, loss caused by earthquake events. In recent years, the focus of community earthquake preparedness has shifted towards resilience and thus, includes time requirements for assessing and repairing the built environment. Post-earthquake inspections serve as a starting point for reoccupation and functional recovery of housing, as well as numerous immediate response actions, including temporary housing and structural stabilization measures. Visual inspection of vast building stocks is slowed down by post-earthquake circumstances and, possibly, by limited resources (i.e. inspectors). However, good decision making towards recovery planning requires rapid availability of reliable data on damage and loss.

Currently, tools for rapid loss assessment (RLA) provide first rapid, yet uncertain, information by combining exposure and vulnerability models with ground-motion estimates that are possibly constrained by seismic recordings [1–3]. Although RLA methodologies are well established and offer crucial initial information maps, their global scope and focus on the immediate aftermath prohibit a dynamic adaptation to new localized information that helps reducing the, typically large, uncertainties. With such information becoming increasingly available in the days following an earthquake, uncertainties pertaining to both ground shaking and structural behavior can be reduced. This paper presents a proposal for continuous dynamic updating of the post-earthquake risk assessment in a restricted geographic area by leveraging machine-learning tools.

Machine-learning techniques have been tested in regional seismic risk prediction, based on the assumption that a subset of buildings is representative of a much larger building stock [4]. Acknowledging the need for centralized information on building damage, Loos et al. proposed a geospatial data integration framework using a kriging regression model to find correlations between observed damage and other secondary parameters [5]. Kovačević et al. used random forests to classify buildings in damage states based on inspection results for a subset of buildings [6]. However, as most techniques are entirely data-driven, they require large amounts of inspected buildings or careful prioritization of inspections to arrive at stable predictions.

We propose Gaussian processes to fuse inspection data with an underlying pre-event earthquake risk model to update it and reduce the underlying uncertainties. Pozzi and Wang proposed a similar method for the purpose of predicting the failure probability of individual components in spatially distributed infrastructure systems [7]. The proposal presented in this paper focuses on aggregated statistics for a diverse building stock. The paper starts with a general description of Gaussian processes for classification and its application to earthquake-induced loss of housing capacity. The methodology is applied to a simulated case study in the greater Zurich area showing the potential for a rapid reduction in uncertainty ranges of inhabitable buildings.

2 Method

The proposed method employs an ex-ante regional earthquake risk model to provide immediate predictions of the consequences inflicted by an event. With the information that eventually becomes available within the first few days following an earthquake event, we continuously update the prior earthquake risk model, using Gaussian process classification, to provide refined consequence predictions. First, Gaussian processes for classification are introduced before their applicability to post-earthquake habitability is discussed.

2.1 Gaussian processes for classification

Gaussian Processes (GPs) provide non-parametric distributions over functions that can be used in probabilistic modelling for supervised learning tasks, including regression and classification [8]. Consider an available training set $D = \{(x_i, y_i)|i=1, ..., n\} = (X, y)$, where matrix $\mathbf{X} = [\mathbf{x}_1, ..., \mathbf{x}_n]$ collects the n input points from domain X and the vector $\mathbf{y}$ collects the corresponding observed class labels $y_i \in \{-1, 1\}$, with the task to predict the class membership probability for a set of m test points $\mathbf{X}_* = [\mathbf{x}_{*,1}, ..., \mathbf{x}_{*_m}]$. A latent function f is employed, and conditional on f, the class labels are assumed to be Bernoulli-distributed independent random variables $p(y_i|f_i) = \Phi(y_i f_i)$, where $f_i = f(\mathbf{x}_i)$ and $\Phi(\cdot)$ is the standard normal cumulative distribution function (cdf); and, $\mathbf{f} = [\mathbf{f}_1, ..., \mathbf{f}_n]$ summarizes the latent function values for inputs, $\mathbf{X}$. $\mathcal{GP}$ classification imposes a Gaussian prior on the latent function

$$f(\mathbf{x}) \sim \mathcal{GP}\left(m(\mathbf{x}), k(\mathbf{x}, \mathbf{x}')\right) \tag{1}$$

where $m(\mathbf{x})$ and $k(\mathbf{x},\mathbf{x}')$ are the mean and positive definite covariance function of a GP. Any finite subset of the random variables, whose collection forms a GP, follows a joint multivariate Gaussian distribution. Thus, a random variable $f(\mathbf{x})$ is associated to every $\mathbf{x} \in X$, such that for any finite set of inputs $\mathbf{X} \in X$, the joint distribution $(\mathbf{f}|\mathbf{X})$ follows a multivariate normal distribution with mean vector $\mathbf{m}_0 = [m(\mathbf{x}_1), ..., m(\mathbf{x}_n)]'$ and covariance matrix $\sum$ with entries $\sum_{ij} = k(x_i, y_i)$. Applying Bayes' rule, the posterior distribution over the latent values f can be expressed as

$$p(\mathbf{f}|y, \mathbf{X}) = \frac{1}{Z} p(\mathbf{f} \mid \mathbf{X}) \prod_{i=1}^{n} p(y_i|f_i) \tag{2}$$

where $Z = p(\mathbf{f}|\mathbf{X}) = \int p(\mathbf{y}|\mathbf{f})\, p(\mathbf{f}|\mathbf{X}) d\mathbf{f}$ is the marginal likelihood. For predictions, we then marginalize latent variables over the training set to evaluate the posterior of the latent function at the test points, $\mathbf{X}_*$.

$$p(\mathbf{f}_*|\mathbf{X}_*, \mathbf{y}, \mathbf{X}) = \int p(\mathbf{f}_*|\mathbf{f}, \mathbf{X}_*, \mathbf{X}) p(\mathbf{f} \mid \mathbf{y}, \mathbf{X}) d\mathbf{f} \tag{3}$$

where $p(\mathbf{f}_*|\mathbf{f},\mathbf{X}_*,\mathbf{X})$ is the conditional prior and follows a multivariate normal distribution. Then, by averaging out the test set latent variables one obtains the predictive class membership probability $p(\mathbf{y}_* = 1|\mathbf{X}_*,\mathbf{y},\mathbf{X})$. Because of the non-Gaussian likelihood, the expressions in Eq. 2 and 3 require sampling algorithms (i.e. Markov-Chain Monte-Carlo). An alternative and computationally more efficient option consists in employing Gaussian approximations to the posterior $q(\mathbf{f}|\mathbf{y},\mathbf{X}) \approx p(\mathbf{f}|,\mathbf{y},\mathbf{X})$. Hence, expectation propagation (EP) approximates the Bernoulli likelihood $p(y_i|f_i) = \Phi(y_i f_i)$ iteratively by using a local likelihood in the form of an un-normalized Gaussian function in the latent variable f_i. Thus, the approximate posterior predictive distribution $q(\mathbf{f}_*|\mathbf{X}_*,\mathbf{y},\mathbf{X})$ is expressed as a multivariate normal distribution. An interested reader is referred to Rasmussen and Williams [8] for further details on EP and similar approximate algorithms.

2.2 Link to regional earthquake risk models

Existing regional earthquake risk models vary in multiple aspects, not only because they are tailored to specific regions and the information available, but they also aim to quantify different quantities of interest. However, most models share two common assumptions: (1) damage to buildings, conditioned on one or multiple ground-motion intensity measures, is independent and (2) the logarithm of ground-motion intensity measures from different sites follow a multivariate normal distribution. The apparent similarity with GP classification motivates the use of ground-motion intensity measures as "latent functions", which will be gradually updated based on new information. The proposed framework is intended for post-earthquake application and therefore, is applied to the consequences inflicted by a scenario earthquake. For a building stock of size n, the quantity of interest is the number of buildings that are uninhabitable after an earthquake event $N_{UI} = n - \sum_i^n H_i$, where random variable $H_i \in \{0,1\}$ denotes the habitability status of building i and $H_i = 1$ indicates that this building remained habitable.

Denote by f_i the logarithm of peak ground acceleration (PGA) at site $\mathbf{x}_i$. Similar to conventional fragility functions, η_k denotes the logarithm of the median PGA, which, if exceeded, renders a building of class k as uninhabitable and β_k its logarithmic dispersion. Then, the conditional probability of a building being rendered uninhabitable is $P(H_i=0|f_i) = \Phi((f_i-\eta_k)/\beta_k)$. Ground-motion prediction equations (GMPEs) provide logarithmic mean, within-event and between-event residuals of PGA conditional on a specified magnitude, epicenter and site coordinates. Together with a suitable spatial correlation model, one can specify the mean vector and covariance matrix of the joint multivariate normal distribution $p(\mathbf{f}_*|\mathbf{X}_*)$ [9], where $\mathbf{X}_*$ collects the inputs (i.e. spatial coordinates) for which predictions are made. In contrast to the classic GP classification problem, a seismic network at locations $\mathbf{X}_s$ collects noisy measurements $\mathbf{z}_s \in \mathbb{R}$ of the function f. Assuming independent and normally distributed noise, the posterior predictive distribution $p(\mathbf{f}_*|\mathbf{X}_*,\mathbf{z}_s,\mathbf{X}_s)$ is analytically tractable and itself a multivariate normal distribution (see [10] for a detailed treatment in the context of shake maps). Thus, by sampling a large number of realizations from this distribution and subsequently from the conditionally

independent Bernoulli distributions $P(H_j|f_j)$, we obtain a first rapid estimate of the aggregated number of uninhabitable buildings $N_{U|}|\mathbf{z}_s$. Note that dependence on the inputs is suppressed to lighten the notation.

The habitability status $\mathbf{y}$ of inspected buildings $\mathbf{X}$ is accumulated from inspections reports in days after the earthquake. By applying the EP algorithm it is possible to derive an updated approximate posterior predictive distribution, $q(\mathbf{f}_{**}|\mathbf{X}_{**},\mathbf{y},\mathbf{z}_s,\mathbf{X}_s)$, a multivariate normal distribution, as new inspection data is accumulated. Note that the new matrix of test inputs, $\mathbf{X}_{**}$, excludes the inputs of already screened buildings $\mathbf{X}$. By applying the above-mentioned sampling scheme and adding the screened buildings that were assessed as uninhabitable we obtain increasingly constrained estimates of $N_{U|}|\ \mathbf{y},\ \mathbf{z}_s$.

3 Case-study

Sections 3.1 and 3.2 introduce the layout of the case-study and the information and earthquake hazard and risk models that are available prior to the earthquake event. Section 3.3 presents the considered scenario earthquake event, the event-specific information that is available in the first ten days after the event, and the hidden data-generating process used to simulate this dataset. Notably, the data-generation process in the scenario event uses earthquake hazard and risk models different from those used to formulate the pre-event earthquake risk prediction. Section 3.4 updates the prior model with the event-specific information to predict the number of uninhabitable buildings.

3.1 Layout and information available prior to the event

The area of interest, illustrated in Fig. 1a, covers 22 zip-codes of the greater Zurich area in Switzerland. We focus on about 34'000 ordinary residential buildings, i.e. buildings with less than 10 stories and with a primary residential use. Pre-event information covers the spatial coordinates, the construction year and the number of stories of every building [11]. The building stock comprises about 25'000 buildings that were built before 1980 as shown in Fig. 1b. The majority of the buildings are between 3 and 5 stories high, as shown in Fig. 1c. Whereas those features are available or can be derived from information in public databases, neither the corresponding models used for the prior regional earthquake risk model, presented in Section 3.2, nor the models used to generate the event-specific dataset, discussed in Section 3.3, are tailored to this specific region and building stock. Thus, results are not necessarily realistic outcomes for such an event occurring in the greater Zurich area.

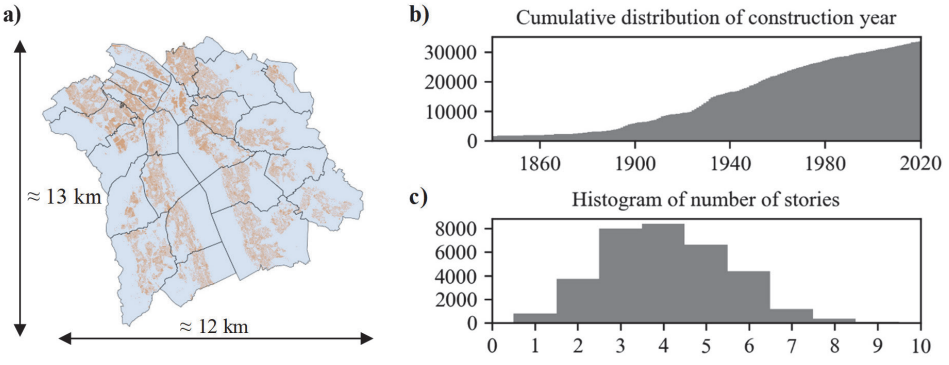

Figure 1. a) Region of interest with delimitation of the zip-codes and locations of about 34'000 individual buildings; b) cumulative distribution of the building construction year parameter (c) histogram of the building story height parameter

3.2 Regional earthquake risk model available ex-ante

The regional risk model, assumed to be available prior to the considered earthquake scenario, categorizes buildings into six classes: unreinforced masonry buildings with either wooden floors or stiff floors (two classes), and reinforced-concrete buildings with a shear-wall or a moment-frame lateral force resisting system that have been constructed before or after the existence of seismic design guidelines (four classes). The first two classes are further divided into low-rise (1-2 stories) and mid-rise (3-5 stories) buildings, whereas for the latter four classes we consider low-rise, mid-rise and high-rise (6 stories or higher) buildings, resulting in a total of 16 subclasses. For every building subclass $k \in [1, 2, ..., 16]$ the set (η_k, β_k) states the parameters of the log-normally distributed building vulnerability functions with respect to the uninhabitable post-earthquake performance state in terms of (logarithm of) PGA, as defined in Section 2.2.

Random fields of PGA are simulated using the GMPE of Akkar and Bommer [12] together with the spatial correlation model of Esposito and Iervolino [9]. Since the true classes of buildings are not known, an expert-knowledge-based model is employed to associate a building class to every building, depending on its construction year and the number of stories. The parameters (η_k, β_k) are based on building vulnerability distributions that have been compiled in the Syner-G project [13] and state the probability of exceeding a set of four discrete damage states (from slight to heavy/complete damage) conditional on PGA. We estimated (η_k, β_k) by assuming that all buildings with damage exceeding slight damage and an additional 10 % of all buildings with slight damage are uninhabitable.

3.3 Scenario earthquake event

A scenario earthquake with a magnitude of 5.8 and an epicenter located approximately 4km to the closest buildings is considered and illustrated in Fig. 2a. Five seismometers within 50 km of the epicenter provide records of the event. After the earthquake strikes, a hotline and a web-based service is made available, such that residents can report damage and request a safety screening. Engineering resources are rapidly briefed to start with the safety screening process. In this process, inspection teams gather information on building classes and assess the habitability status. Fig. 2b shows the cumulative number of buildings screened during the first 10 days after the event, whereas Fig. 2c indicates how many buildings have been screened in each of the 22 zip-codes 10 days after the event.

The hidden data-generating models used to produce this simulated dataset, labeled as the "true" realization, are deliberately chosen to differ from the models available for earthquake risk prediction (Section 3.2). Most notably, a set of four ground-motion intensity measures is used to derive the habitability status of buildings, instead of PGA. The building stock is categorized using building classes defined in the global risk model [3] and a class is associated to all buildings depending on their construction age and the number of stories. We generate one realization of PGA and spectral accelerations at fundamental periods of 0.3, 0.6 and 1.0 seconds using the GMPE of Bindi et al. [14], the spatial cross-correlation model of Markvidha et al. [15] for the within-event residuals and of Baker and Cornell [16] for cross-correlation of between-event residuals. Employing the fragility curves given by Silva et al. [3], the damage state of each building is estimated. Then, we assume that occupants of all buildings that sustained at least slight damage request a safety screening. Of all buildings with a request, we assume 15 % of the buildings with slight damage are uninhabitable, together with all buildings having a damage state exceeding slight damage. At the beginning of every day, available inspection teams are randomly assigned to a building with an open request for safety screening. After completing the first inspection, each team continues to inspect the geographically closest building having an open request.

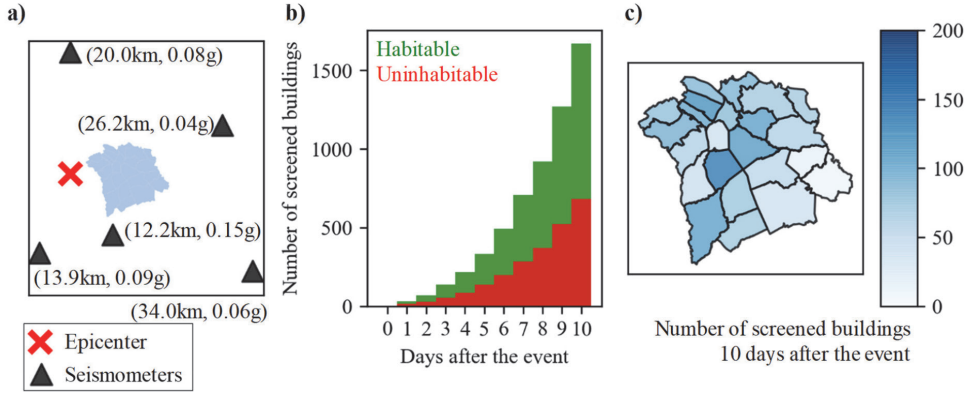

Figure 2. a) Epicenter of the considered scenario earthquake of magnitude 5.8 and locations of seismic network stations, their epicentral distance and the measured peak ground acceleration, b) Cumulative number of screened buildings in the entire region of interest over the first 10 days after the event, c) The number of buildings per zip-code that have been screened 10 days after the event

3.4 Dynamic updating of the predicted number of uninhabitable buildings

Using the method described in Section 2, we predict the number of uninhabitable buildings N_{UI} in the entire region of interest and examine how these predictions evolve over the first 10 days after the event. We denote the aggregated inspection data (see Fig. 2b) obtained until and including day t as $\mathbf{y}_{0:t}$ and the prediction derived using the posterior of the latent function conditional on this data as $N_{UI}|\mathbf{y}_{0:t}, \mathbf{z}_s$. The solid line in Fig. 3a illustrates $E[N_{UI}|\mathbf{y}_{0:t}, \mathbf{z}_s]$ over the first 10 days, e.g. $t \in [0, ..., 10]$. Furthermore we state the α-quantile as $q_\alpha[N_{UI}|\mathbf{y}_{0:t}, \mathbf{z}_s]$ and the 90 % credibility interval as the range between $q_{0.95}$ and $q_{0.05}$. The "true" realization, simulated with the model described in Section 3.3, is indicated with the dashed black line and corresponds to 7'500 uninhabitable buildings. On day 0, immediately following the event, the earthquake risk prediction is based on the recorded PGA values only (see Fig. 2a) and the credibility interval spans from 7'000 up to 25'000 uninhabitable buildings, with an expected value around 16'000 uninhabitable buildings (out of the approximately 34'000 buildings in the considered region). In the following days, leveraging the information from rapid visual safety screening, the uncertainty in the predictions is reduced and the trend tends towards the "true" realizations. Panel (b) of Fig. 3 illustrates the same predictions as a function of the cumulative number of screened buildings.

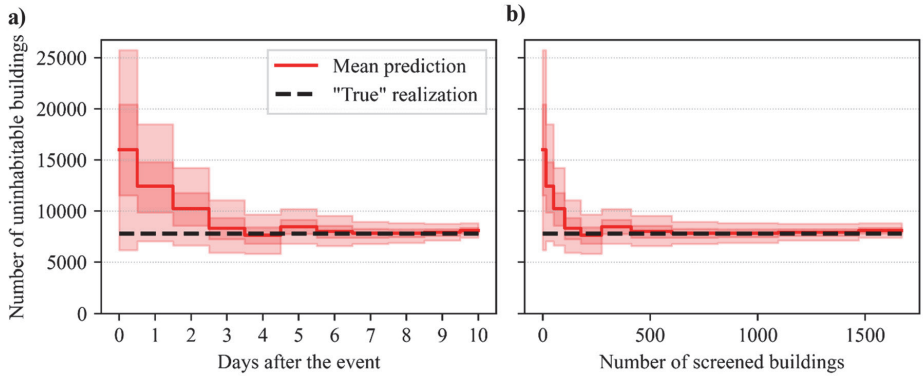

Figure 3. Evolution of predictions of number of uninhabitable buildings $N_{UI}|\mathbf{y}_{0:t},\mathbf{z}_s$ as a function: a) days t after the event, b) cumulative number of screened buildings available for inference. Light and dark red shaded intervals indicate the 90 % and 50 % credibility interval, respectively

Instead of predicting the outcome for the entire region, the proposed method also delivers predictions on a zip-code level, as illustrated in Fig. 4. The top, middle and bottom row show the 90 % quantile, the expected value and the 5 % quantile of the relative number of uninhabitable buildings in each zip-code, respectively, for $t \in [0,5,10]$ days after the event, going from left to right. The right side of Fig. 4 illustrates the "true" realization of the ratio of uninhabitable buildings in each zip-code. Whereas for day 0 the predictions are very uncertain, and this ratio might be between 10 % and 80-90 % for almost all zip-codes, we observe that including screening results of the first five days (approximately 300 inspected buildings) already leads to a more precise and accurate spatial pattern.

4. Conclusion

A Gaussian Process based classification is used to reduce the uncertainty ranges of predicted loss of housing capacity in a region affected by an earthquake. Having in mind that this paper presents results for a simulated scenario earthquake, following preliminary conclusions are drawn:

Classification techniques show potential to provide stable and precise predictions of the number of uninhabitable buildings in a fraction of the time required to inspect the entire building stock.

Based on incomplete inspection data from randomly selected buildings, spatially accurate distributions of unsafe buildings are achieved and provide a significant uncertainty reduction with respect to rapid loss assessment based on shake maps.

Gaussian Process classification is robust to inevitable discrepancies between the regional risk model and the underlying unknown behavior of buildings undergoing an earthquake.

The predicted quantity of interest in this paper is chosen to be the habitability of buildings, addressing the loss of regional housing capacity after an earthquake, an important measure of community disaster resilience. However, the proposed framework can be applied to other useful quantities for rapid post-earthquake loss and recovery assessment, such as financial loss or repair effort. Notably, the dependence on the outcome of visual inspection reflects the current state of the art. The framework can, however, ingest post-earthquake damage information from other sources, such as image processing from either drones or satellites or structural health monitoring applications. Finally, the robustness of the framework to inaccurate inspection outcomes and approximate exposure models will be assessed in future work.

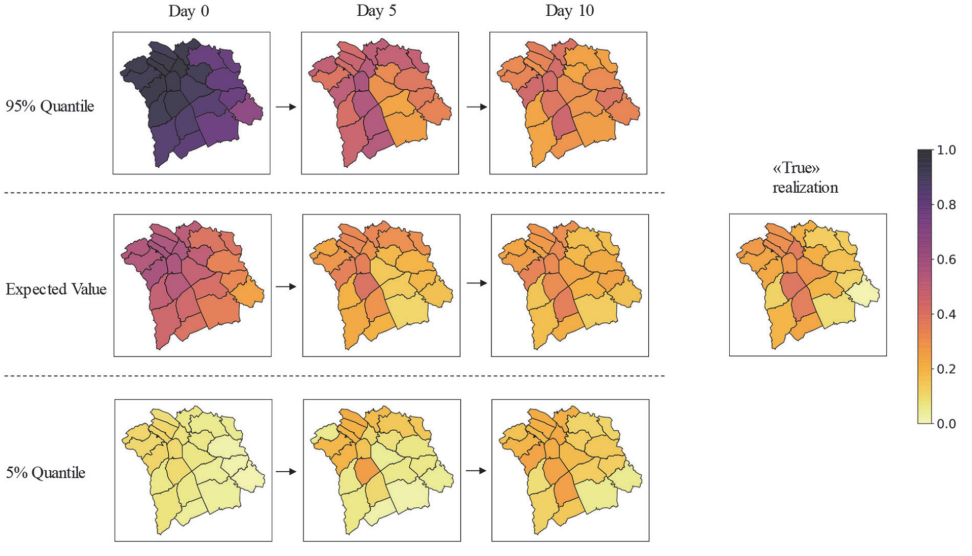

Figure 4. The 95 %-quantile, expected value and 5 %-quantile (from top to bottom) of the ratio of uninhabitable buildings for each zip-code predicted on day 0, and updated with inspection data accumulated until day 5 and day 10 after the event. The right-hand side shows the "true" ratio of uninhabitable buildings in this scenario

Acknowledgements

The research described in this paper was financially supported by the Real-time Earthquake Risk Reduction for a Resilient Europe 'RISE' project, financed under the European Union's Horizon 2020 research and innovation program, under grant agreement No 821115, as well as the ETH Grant (ETH-11 18-1) DynaRisk - "Enabling Dynamic Earthquake Risk Assessment".

References

[1] Wald, D. J., Earle, P. S., Allen, T. I., Jaiwal, K., Porter, K., Hearne, M. (2008). Development of the U.S. Geological Survey's PAGER system (Prompt Assessment of Global Earthquakes for Response), *The 14th World Conference on Earthquake Engineering*, 1–8

[2] Erdik, M., Şeşetyan, K., Demircioğlu, M. B., Hancilar, U., Zülfikar, C. (2011). Rapid earthquake loss assessment after damaging earthquakes, *Soil Dynamics and Earthquake Engineering*, Vol. 31, No. 2, 247–266. doi:10.1016/j.soildyn.2010.03.009

[3] Silva, V., Amo-Oduro, D., Calderon, A., Costa, C., Dabbeek, J., Despotaki, V., Martins, L., Pagani, M., Rao, A., Simionato, M., Viganò, D., Yepes-Estrada, C., Acevedo, A., Crowley, H., Horspool, N., Jaiswal, K., Journeay, M., Pittore, M. (2020). Development of a global seismic risk model, *Earthquake Spectra*, Vol. 36, No. 1_suppl, 372–394. doi:10.1177/8755293019899953

[4] Diana, L., Thiriot, J., Reuland, Y., Lestuzzi, P. (2019). Application of Association Rules to Determine Building Typological Classes for Seismic Damage Predictions at Regional Scale: The Case Study of Basel, *Frontiers in Built Environment*, Vol. 5. doi:10.3389/fbuil.2019.00051

[5] Loos, S., Lallemant, D., Baker, J., McCaughey, J., Yun, S.-H., Budhathoki, N., Khan, F., Singh, R. (2020). G-DIF: A geospatial data integration framework to rapidly estimate post-earthquake damage, *Earthquake Spectra*, Vol. 36, No. 4, 1695–1718. doi:10.1177/8755293020926190

[6] Kovačević, M., Stojadinović, Z., Marinković, D., Stojadinović, B. (2018). Sampling and machine learning methods for a rapid earthquake loss assessment system, *11th U.S. National Conference on Earthquake Engineering*, Earthquake Engineering Research Institute, Los Angeles, CA

[7] Pozzi, M., Wang, Q. (2018). Gaussian Process Regression and Classification for Probabilistic Damage Assessment of Spatially Distributed Systems, *KSCE Journal of Civil Engineering*, Vol. 22, No. 3, 1016–1026. doi:10.1007/s12205-018-0014-x

[8] Rasmussen, C. E., Williams, K. I. (2006). *Gaussian Processes for Machine Learning*, The MIT Press, Cambridge, MA

[9] Esposito, S., Iervolino, I. (2011). PGA and PGV Spatial Correlation Models Based on European Multievent Datasets, *Bulletin of the Seismological Society of America*, Vol. 101, No. 5, 2532–2541. doi:10.1785/0120110117

[10] Worden, C. B., Thompson, E. M., Baker, J. W., Bradley, B. A., Luco, N., Wald, D. J. (2018). Spatial and spectral interpolation of ground-motion intensity measure observations, *Bulletin of the Seismological Society of America*, Vol. 108, No. 2, 866–875. doi:10.1785/0120170201

[11] Amt für Raumentwicklung. (n.d.). Geografisches Informationssystem des Kantons Zürich (GIS-ZH), *GIS-Browser*, from http://maps.zh.ch, accessed 20-2-2020

[12] Akkar, S., Bommer, J. J. (2010). Empirical Equations for the Prediction of PGA, PGV, and Spectral Accelerations in Europe, the Mediterranean Region, and the Middle East, *Seismological Research Letters*, Vol. 81, No. 2, 195–206. doi:10.1785/gssrl.81.2.195

[13] Pitilakis, K., Crowley, H., Kaynia, A. M. (2014). *SYNER-G: Typology Definition and Fragility Functions for Physical Elements at Seismic Risk*, *11* (Vol. 27)

[14] Bindi, D., Luzi, L., Massa, M., Pacor, F. (2010). Horizontal and vertical ground motion prediction equations derived from the Italian Accelerometric Archive (ITACA), *Bulletin of Earthquake Engineering*, Vol. 8, No. 5, 1209–1230. doi:10.1007/s10518-009-9130-9

[15] Markhvida, M., Ceferino, L., Baker, J. W. (2018). Modeling spatially correlated spectral accelerations at multiple periods using principal component analysis and geostatistics, *Earthquake Engineering & Structural Dynamics*, Vol. 47, No. 5, 1107–1123. doi:10.1002/eqe.3007

[16] Baker, J. W., Cornell, A. (2006). Correlation of Response Spectral Values for Multicomponent Ground Motions, *Bulletin of the Seismological Society of America*, Vol. 96, No. 1, 215–227. doi:10.1785/0120050060